

Keywords: renal cancer; diffusion-weighted MRI; multiphase contrast-enhanced MRI; sunitinib

Diffusion-weighted and multiphase contrast-enhanced MRI as surrogate markers of response to neoadjuvant sunitinib in metastatic renal cell carcinoma

N Bharwani^{*1}, M E Miquel^{2,3}, T Powles⁴, P Dilks¹, A Shawyer¹, A Sahdev¹, P D Wilson⁵, S Chowdhury⁶, D M Berney⁷ and A G Rockall¹

¹Department of Radiology, Barts Health NHS Trust, St Bartholomew's Hospital, King George V Building, West Smithfield, London EC1A 7BE, UK; ²Department of Clinical Physics, Barts Health NHS Trust, St Bartholomew's Hospital, 4th Floor Dominion House, 60 St Bartholomew's Close, London EC1A 7BE, UK; ³Barts and the London NIHR Cardiovascular Biomedical Research Unit, Centre for Advanced Cardiovascular Imaging, Queen Mary University of London, Bonner Road, London E2 9JX, UK; ⁴Barts Cancer Institute, Experimental Cancer Medicine Centre, Queen Mary University of London, Charterhouse Square, London EC1M 6BQ, UK; ⁵Department of Medical Oncology, St Bartholomew's Hospital, 7th Floor Gloucester House, London EC1A 7BE, UK; ⁶Department of Medical Oncology, Guys and St Thomas' NHS Foundation Trust, Great Maze Pond, London SE1 9RT, UK and ⁷Barts Cancer Institute, Molecular Oncology and Cellular Pathology, Queen Mary University of London, Charterhouse Square, London EC1M 6BQ, UK

Background: Current imaging criteria for categorising disease response in metastatic renal cell carcinoma (mRCC) correlate poorly with overall survival (OS) in patients on anti-angiogenic therapies. We prospectively assess diffusion-weighted and multiphase contrast-enhanced (MCE) MR imaging (MRI) as markers of outcome.

Methods: Treatment-naïve mRCC patients on a phase II trial using sunitinib completed an MRI substudy. Whole-tumour apparent diffusion coefficient (ADC) maps and histograms were generated, and mean ADC and AUC_{low} (proportion of the tumour with ADC values lying below the 25th percentile of the ADC histogram) recorded. On MCE-MRI, regions of interest were drawn around the most avidly enhancing components to analyse enhancement parameters. Baseline ($n=26$) and treatment-related changes in surviving patients ($n=20$) were correlated with OS. Imaged metastases were also analysed.

Results: Forty-seven per cent of the patients showed significant changes in whole-tumour mean ADC following therapy, but there was no correlation with outcome. Patients with a high baseline AUC_{low} and greater-than-median AUC_{low} increase had reduced OS (HR = 3.67 (95% confidence interval (CI) = 1.23–10.9), $P=0.012$ and HR = 3.72 (95% CI = 0.98–14.21), $P=0.038$, respectively). There was no correlation between MCE-MRI parameters and OS. Twenty-eight metastases were analysed and showed positive correlation with primary tumour mean ADC for individual patients ($r=0.607$; $P<0.001$).

Conclusion: Primary RCC ADC histogram analysis shows dynamic changes with sunitinib. Patients in whom the tumour ADC histogram demonstrated high baseline AUC_{low} or a greater-than-median increase in AUC_{low} with treatment had reduced OS.

*Correspondence: Dr N Bharwani; E-mail: Nishat.Bharwani@Imperial.nhs.uk

Received 8 May 2013; revised 17 November 2013; accepted 21 November 2013; published online 24 December 2013

© 2014 Cancer Research UK. All rights reserved 0007–0920/14

Treatment of metastatic renal cell carcinoma (mRCC) has been revolutionised by targeted therapies such as sunitinib, a multi-targeted tyrosine kinase inhibitor with a broad spectrum of activity, which focuses mainly on vascular endothelial growth factor receptors which play a role in both tumour angiogenesis and tumour cell proliferation. These therapies have increased mean survival to over 2 years compared with less than 1 year previously and are now considered standard of care in mRCC (Motzer *et al*, 2007, 2009).

Current imaging criteria for categorising disease response is with RECIST (Response Evaluation Criteria in Solid Tumors) v1.1. However, response by RECIST, based on target lesion size, does not correlate with overall survival (OS) in mRCC patients treated with sunitinib (Kontovinis *et al*, 2009). Alternative imaging-based response parameters have been evaluated, including lesion texture, size and attenuation on contrast-enhanced computed tomography (CT) and glucose metabolism on positron emission tomography/CT, with variable success (Hahn *et al*, 2008; Han *et al*, 2010; Nathan *et al*, 2010; Thiam *et al*, 2010; Smith *et al*, 2010a,b; Goh *et al*, 2011; Krajewski *et al*, 2011; Smith *et al*, 2011). There remains a lack of biological and radiological markers that reliably predict (i) response to sunitinib early in the course of treatment and (ii) which patients will develop early resistance to treatment.

Diffusion-weighted (DW) and dynamic contrast-enhanced (DCE) MR imaging (MRI) are imaging techniques that probe tumour physiology. Diffusion-weighted MRI explores the Brownian motion of water, which is restricted by interactions with cell membranes and macromolecules in tissues, and is quantified by the apparent diffusion coefficient (ADC) (Koh and Collins, 2007). Increased tissue cellularity, as seen in some tumours, restricts diffusion, resulting in low ADC values. Early change in DW-MRI/ADC following treatment has been proposed as a potential biomarker for assessment of response in other cancers (Harry *et al*, 2008; Jung *et al*, 2011; Kyriazi *et al*, 2011). Whole-tumour mean ADC histogram analysis can evaluate heterogeneity within a tumour by classifying regions of different cellularity and micro-environments (Kyriazi *et al*, 2011; Nowosielski *et al*, 2011; Pope *et al*, 2011). Previous studies have used quantitative DCE-MRI to assess contrast material kinetics within a tumour, reflecting the vascularity of the tissue. These studies have suggested that changes in the volume transfer constant of contrast agent (K_{trans}) can be used as a pharmacodynamic biomarker in patients on anti-angiogenic therapy (Morgan *et al*, 2003; Stevenson *et al*, 2003; Liu *et al*, 2005; Mross *et al*, 2005; Flaherty *et al*, 2008; Hahn *et al*, 2008; Notohamiprodjo *et al*, 2010). Multiphase contrast-enhanced (MCE) MRI allows semiquantitative parameters such as maximum relative enhancement (SI_{rel}) and relative wash-in rate (WIR_{rel}) to be more readily measured in everyday clinical practice, but these have not previously been evaluated in the context of response to sunitinib therapy in mRCC.

The primary objective of this translational study was to assess whether sunitinib therapy was associated with sequential changes in the unresected treatment-naive primary renal tumour in patients recruited to an imaging substudy of a phase II trial (SUMR NCT01024205) and to evaluate whether these changes correlated with OS. We hypothesised that response to treatment, as defined by improved OS, would correlate with:

- (i) an increase in ADC of the whole primary tumour volume due to apoptosis and
- (ii) a reduction in primary tumour vascularity due to anti-angiogenic effects.

Our secondary objectives were:

- (i) to evaluate novel methods of histogram analysis in the primary tumour and

- (ii) to assess treatment-related diffusion and/or perfusion alterations in the imaged metastases.

PATIENTS AND METHODS

Study design. The study protocol was approved by the research ethics committee and all patients gave written consent.

All patients with newly diagnosed mRCC referred to our tertiary uro-oncology centre were considered for inclusion in the prospective phase II trial (SUMR NCT01024205). The primary endpoint of the SUMR trial was to assess the clinical benefit of upfront sunitinib in Memorial Sloan-Kettering Cancer Centre (MSKCC) intermediate- and poor-risk patients who had not had nephrectomy (Powles *et al*, 2011). Outcome data were available for OS with a follow-up period of 31.9 months (range 8.3–39.8 months).

Key inclusion criteria were histopathologically confirmed clear cell RCC with metastases, judged by the treating clinician to potentially derive benefit from sunitinib. Key exclusion criteria included previous treatment for mRCC and contra-indication to MRI.

Patients. Between January 2008 and February 2010, 30 consecutive patients (23 men, 7 women) with untreated mRCC were recruited to the MRI substudy. Inclusion in this substudy required the absence of contra-indications to MRI and patient consent for additional imaging. MR imaging results did not influence treatment decisions.

Four patients were excluded because they did not complete post-treatment imaging for reasons other than progressive disease leading to death (unable to schedule second MRI $n=2$; declined second scan $n=2$). Patient demographics are given in Table 1.

Baseline MRI was performed on all 26 patients. Six patients died from progressive disease before completion of three treatment cycles. Radiological response data (pre- and post-treatment imaging) was therefore available in 20 patients. Three patients recruited to the study had an incomplete set of b -values at baseline (only $b=0$ and $b=1000 \text{ smm}^{-2}$). To avoid possible data contamination by these differences in baseline DW-MRI acquisition, DW-MRI analysis has been performed following exclusion of the three patients with differing baseline DW-MRI acquisitions. Multiphase contrast-enhanced MRI was performed using the same protocol in all patients.

Figure 1 provides a flow diagram to illustrate the imaging performed in patients recruited to the substudy.

Treatment schedule. Patients were treated with three cycles of sunitinib until progression or withdrawal (50 mg daily for 4 weeks with a 2-week break between cycles). Doses were reduced to 37.5 mg and subsequently 25 mg in the face of toxicity (grade 3 or more). Interval debulking nephrectomy was offered to patients after the MRI study (following three treatment cycles). Following surgery, patients continued sunitinib treatment until progression by RECIST v1.1. The role of nephrectomy in metastatic disease is controversial and is under evaluation in studies such as SUMR.

Figure 2 provides a study schema to illustrate the relationship between neoadjuvant therapy, imaging and surgery in the patient cohort.

MR imaging protocol. MR imaging was acquired pre-treatment and following three treatment cycles on a 1.5-Tesla Philips Achieva MRI scanner (Philips Medical Systems, Best, The Netherlands) with a four-element phased array coil. The second MRI study was performed off treatment during the second week, following the completion of cycle 3 and before nephrectomy (day 10 ± 2 off treatment; see Figure 2). Hyoscine butylbromide (Buscopan; Boehringer, Ingelheim, Germany; 20 mg intravenously) was

Table 1. Patient demographics and characteristics at diagnosis

Number of patients	26
Age (years)	61.5 ± 10.3 (range 38–78)
Gender	
Male	21
Female	5
MSKCC prognostic risk	
Intermediate	12
Poor	14
Metastatic sites	
Lung	16
Liver	5
Bone	8
Lymph nodes	14
Adrenal	4
Other	8
Clear cell tumour grade	
1–2	14
3–4	12
Median OS, months	13.6
Median PFS, months	6.4
Median follow-up, months	31.9 (range 8.3–39.8)
Abbreviations: MSKCC=Memorial Sloan-Kettering Cancer Centre; OS=overall survival; PFS=progression-free survival.	

slice gap, 1 mm; field of view (FOV), 375 mm; rectangular FOV (RFOV), 75%; 3 signal averages; 400 × 512 matrix) and axial T_1 -weighted fast field-echo MRI (TR, 150–225 ms; TE, 5 ms; flip angle, 80°; slice thickness, 6 mm; slice gap, 1 mm; FOV, 375 mm; RFOV, 75%; 2 signal averages; 256 × 400 matrix).

Diffusion-weighted-MR images were obtained using a free-breathing multislice spin-echo echo-planar imaging sequence (TR, range 6000–7000 ms; TE, 67 ms; EPI factor, 60; slice thickness, 6 mm; slice gap, 1 mm; FOV, 400–450 mm; RFOV, 75%; 3 signal averages; 256 × 256 matrix). Six motion-probing gradients with b -values of 0, 100, 200, 500, 750 and 1000 $s\text{ mm}^{-2}$ were applied in three orthogonal directions and trace images were synthesised for each b -value using the mean of three orthogonal directions. Apparent diffusion coefficient maps were calculated on a pixel-by-pixel basis using a mono-exponential fit excluding $b=0$ from the calculation to eliminate perfusion effects (Padhani *et al*, 2009). Average DW-MRI acquisition time was 8 min.

The variability of the free-breathing multislice DW-MRI sequence was previously measured in a phantom and volunteer study at our centre (Miquel *et al*, 2012). *In vivo* repeatability for renal ADC measurements demonstrated a coefficient of reproducibility of 7.9% for three-dimensional volumes of interest, but up to 24% for single regions of interest (ROI) in the abdomen.

Multiphase contrast-enhanced MRI was performed with volumetric fat-suppressed, spoiled gradient-echo T_1 -weighted acquisitions in the coronal plane (TR, 4 ms; TE, 1.9 ms; flip angle, 10°; slice thickness, 6 mm; slice gap, 1 mm; FOV, 400–450 mm; RFOV, 75%; 2 signal averages; 256 × 256 matrix) before and at 60, 120, 180, 240, 300, 360 and 420 s after controlled pump intravenous injection of 10 ml of 0.5 mmol ml⁻¹ gadoteric acid (Dotarem; Guerbet, Villepinte, France) at a rate of 3 ml s⁻¹. The total acquisition time including pre-contrast imaging was 450 s. Images were reconstructed in the axial plane for semiquantitative analysis.

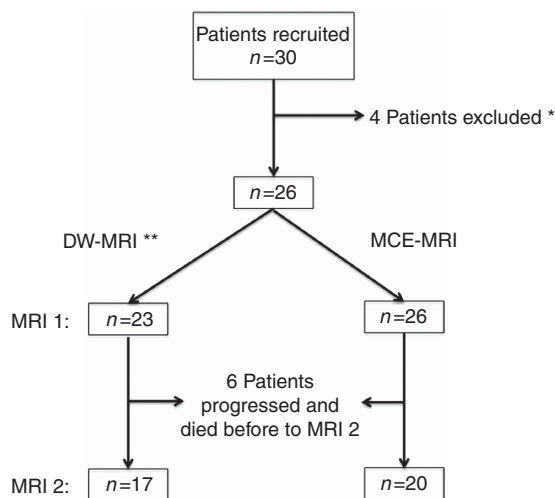


Figure 1. Flow diagram illustrating the imaging performed in the MRI substudy cohort. *Four patients were excluded from the study because they did not complete post-treatment imaging for reasons other than progression. **In three patients, the initial DW-MRI study was performed using only two b -values. These patients have been excluded from the DW-MRI analysis but remain in the MCE-MRI analysis.

administered before image acquisition to reduce artefact related to bowel movement. For all sequences, the field of view was optimised to include the entire primary renal tumour. The following morphological sequences were obtained: axial T_2 -weighted turbo spin-echo MRI (repetition time (TR), range 1500–1750 ms; echo time (TE), 100 ms; turbo factor, 28; slice thickness, 6 mm;

Image analysis. Diffusion-weighted-MR images were analysed using OsiriX (Pixmeo SARL, Bernex, Switzerland) software by a single reader (2 years of body MRI fellowship experience), blinded to clinical outcome. The whole primary tumour was segmented on the ADC map, in conjunction with $b=1000\text{ s mm}^{-2}$ and T_2 -weighted sequences. The largest possible ROI was drawn on each slice containing primary tumour, without contamination from adjacent tissues (Figure 3). OsiriX software calculated the tumour volume and pixel-by-pixel mean ADC values for the entire volume. Mean ADC values were exported into Microsoft Excel software for whole-tumour mean ADC calculation and generation of per patient volume-corrected ADC histograms (bin width $50 \times 10^{-6}\text{ mm}^2\text{ s}^{-1}$). The histogram-derived parameter was the AUC_{low} : the proportion of the tumour with ADC values lying below the 25th percentile point of the ADC histogram (the pixel ADC value below which 25% of all tumour ADC values lie) after the highest and lowest 1% of ADC values were discarded to remove artefact. AUC_{low} represents the most restricted, and probably the most cellular, components of the tumour (see Figure 4 for AUC_{low} derivation).

Multiphase contrast-enhanced-MR images were analysed using the MR Breast Imaging package of Philips Extended Workspace (R 2.6.3.2, 2009, Philips Healthcare, Best, The Netherlands) by two readers (each with 1 year of body MRI experience) in consensus following training by an experienced (10 years) MRI reader, all blinded to clinical outcome. The most avidly enhancing solid tumour component was identified on the baseline study using the coloured parametric map and a circular ROI (diameter > 3 mm) was manually drawn. This ROI was then copied to the same anatomical position on the post-treatment study, visually matching the same tumour region. Computer software automatically calculated the following parameters:

$$SI_{rel} = (SI_{max} - SI_0) / SI_0 \times 100 \text{ (maximal tissue enhancement from baseline).}$$

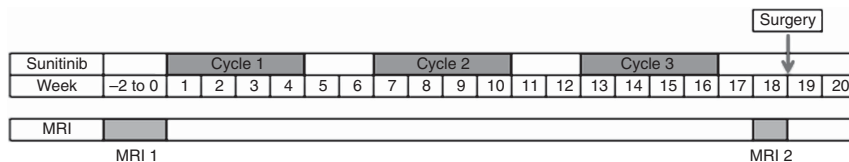


Figure 2. Magnetic resonance imaging substudy schema illustrating the relationship between neoadjuvant therapy, MR imaging and surgery in patients recruited to the MRI substudy. The second MRI study was performed in the second week off treatment following cycle 3 of sunitinib and before nephrectomy.

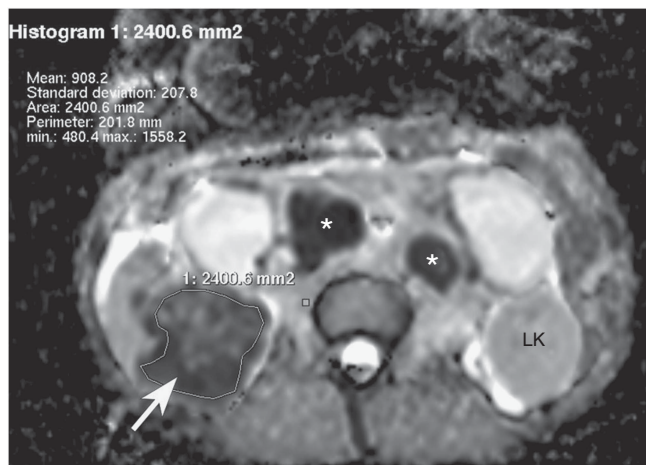


Figure 3. Region of interest placement. Axial section through a right-sided renal cell carcinoma (white arrow) showing the placement of a ROI within the low ADC tumour. Care is taken to sample only tumour tissue without contamination from adjacent normal tissues. Workstation-generated analysis gives a mean ADC value of $0.91 \times 10^{-3} \text{ mm}^2 \text{ s}^{-1}$ for the tumour at this level. This section also demonstrates involved retroperitoneal nodes (white stars), which return lower ADC values than the primary tumour. LK = left kidney.

Wash-in rate (WIR) = $(SI_{\text{max}} - SI_0) / \text{time (s)}$ (velocity of tissue enhancement).

Software-derived parameters were also used to calculate the WIR_{rel} to overcome day-to-day variations based on coil placement and magnetic performance.

$WIR_{\text{rel}} = SI_{\text{rel}} / \text{time (s)}$ (SI_{max} = maximal tissue signal intensity following contrast medium administration; SI_0 = tissue signal intensity on non-enhanced T_1 -weighted sequence; time = time to maximal enhancement).

The volume of necrosis in each primary tumour (defined as the volume of non-enhancing tissue with corresponding high T_2 signal intensity) was calculated using OsiriX software (Rosset *et al*, 2004). Because of the heterogeneity of the primary tumour on T_2 and the presence of internal high signal intensity on T_1 , ROIs were defined on consecutive axial T_2 -weighted images by matching areas of high T_2 signal intensity with regions of non-enhancement on the subtracted MCE-MR images. Separate volumes of necrosis were summed to give a total necrotic volume that was expressed as a percentage of the primary tumour volume.

Metastatic deposits. The imaging volume was optimised to include the entire primary renal tumour. Whole-body imaging was not performed and, therefore, the majority of metastases identified on the patient's staging CT (e.g., pulmonary deposits) were not assessed on MRI.

Metastatic deposits were defined as lesions $>1 \text{ cm}$ in diameter (or $>1.5 \text{ cm}$ in short axis for nodes) that had typical CT and MRI appearances for RCC metastases (Griffin *et al*, 2009). Inferior vena cava (IVC) thrombus was included in analysis where

enhancement on MCE-MRI indicated tumour rather than bland thrombus.

Mean ADC values were obtained from a single ROI on the central slice through each lesion (the majority were too small for volume assessment) at baseline and following three treatment cycles.

Standard response assessment. Standard response was classified according to RECIST v1.1, as specified in the clinical phase II trial protocol. Contrast-enhanced CT of the chest, abdomen and pelvis (100 ml Omnipaque350 (GE Healthcare, Milwaukee, WI, USA) administered at 3.5 mls^{-1}) was performed at baseline and after every three cycles of treatment. Progression-free survival (PFS) was not used as an endpoint in this study, as 36% of patients have been shown to progress during the surgery-related break when treated with upfront sunitinib before planned nephrectomy (as in the SUMR protocol) and, therefore, PFS does not act as a good surrogate marker (Powles *et al*, 2011). Because of the lack of second-line therapy in the United Kingdom at the time of the study, OS was considered the most robust endpoint.

Statistical analysis. Statistical analysis was conducted using STATA software (Statacorp LP, College Station, TX, USA). Descriptive statistics were used to analyse parameters. Overall survival was analysed using the Kaplan–Meier (KM) method with patients being separated into two groups, those above and those below the median, for each parameter. Comparison of groups was conducted using the log-rank test. Correlation coefficients (Pearson's product-moment correlation coefficient) were used to compare the relationship between groups.

A level of $P < 0.05$ was used to assess for the significance of the results obtained and there has been no correction for multiple comparisons.

RESULTS

Best-response evaluation by RECIST v1.1 in this MSKCC intermediate- and poor-risk population showed partial response in 2 patients (8%), stable disease in 16 patients (61%) and progressive disease in 8 patients (31%). Overall survival for all patients was 13.6 months (95% confidence interval (CI): 4–22.7).

Primary tumour

Morphological analysis. Characteristics of the primary tumour at baseline and after three cycles of treatment in patients who had sequential scans were analysed (Table 2). Interval changes in primary tumour volume ranged from -70.7 to $+57.8\%$ (mean, -18.3 ± 35.1) and changes in the percentage of primary tumour necrosis ranged from -14.1 to $+46.2\%$ (mean, 14.0 ± 15.8). Patients who had a tumour volume below median at baseline had a prolonged survival compared with those with a baseline tumour volume above median (OS 28.3 months compared with 4.0 months; $P = 0.017$). The percentage change in tumour volume with treatment did not correlate with survival ($P = 0.087$). Those patients in whom the change in the percentage necrosis was below

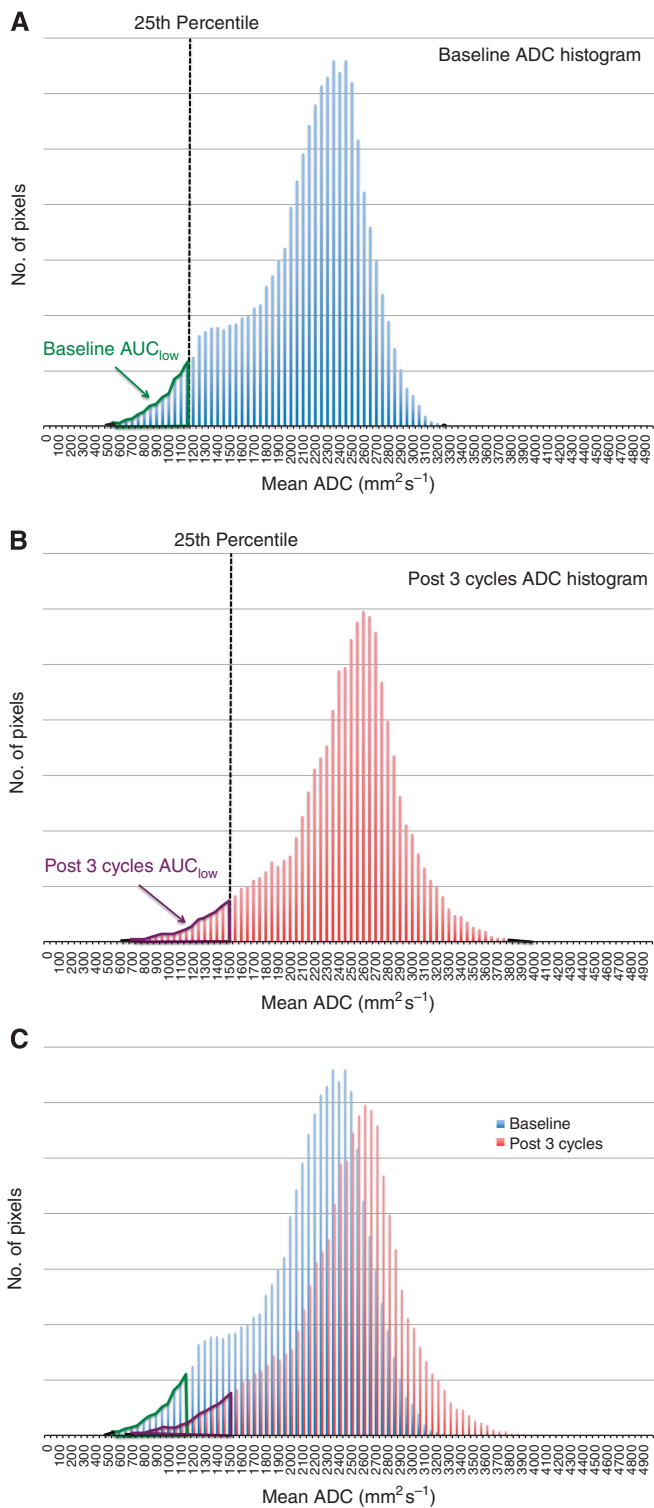


Figure 4. ADC histogram analysis: derivation of AUC_{low} . Pre- and post-treatment ADC histograms were generated from pixel-by-pixel mean ADC measurements from the entire tumour volume. The highest and lowest 1% of ADC values (the tails of the bell-shaped curve) were discarded to remove artefact (blacked out regions). The 25th percentile point of the histogram range, the pixel ADC below which 25% of all tumour ADC values lie, was calculated for each curve and the proportion of the tumour with ADC values lying below this point was measured (AUC_{low} ; outlined in green at baseline (A) and in purple following three treatment cycles (B)). (C) Pre- and post-treatment ADC histograms displayed on the same axis demonstrating the treatment-related changes in the histogram and AUC_{low} .

Table 2. Primary tumour MRI characteristics at baseline and after three treatment cycles in the full cohort

Parameter	Baseline	After three cycles	P-value
Number of patients	26	20	NA
Mean primary tumour volume ($\times 10^3 \text{ mm}^3$)	0.60 ± 0.73	0.58 ± 0.81	0.11
Mean primary tumour necrosis (%)	15.70 ± 16.60	27.20 ± 17.50	<0.001
Mean tumour ADC ($\times 10^{-3} \text{ mm}^2 \text{ s}^{-1}$) ^a	1.31 ± 0.34	1.46 ± 0.30	0.10
Mean AUC_{low} ^a	22% (IQR: 14.9–27.1%)	15.6% (IQR: 11.2–24.0%)	0.16
Primary tumour WIR (si s^{-1})	17.27 ± 10.4	22.2 ± 30.47	0.54
Primary tumour WIR_{rel} ($\% \text{ s}^{-1}$)	2.53 ± 1.06	2.10 ± 1.11	0.22
Primary tumour SI_{rel} (%)	169%	131%	0.09

Abbreviations: ADC = apparent diffusion coefficient; DW-MRI = diffusion-weighted MRI; MRI = magnetic resonance imaging; NA = not applicable; SI_{rel} = maximum relative enhancement; WIR = wash-in rate; WIR_{rel} = relative wash-in rate.
^aDW-MRI analysis performed on 23 patients at baseline and 17 patients following 3 treatment cycles.

the median (−14.1 to +4.6% change) had a trend towards prolonged OS compared with those above median (+8.5 to +46.2% change; $P = 0.058$).

Diffusion-weighted MRI parameters. Analysis of ADC histograms in the 23 patients at baseline demonstrated marked tumour heterogeneity (skewness 0.56, kurtosis 3.63). There was no significant change in skewness or kurtosis of the ADC histogram with treatment. Whole-tumour mean ADC values varied between 0.80 and $2.1 \times 10^{-3} \text{ mm}^2 \text{ s}^{-1}$. We evaluated whether primary tumour DW-MRI parameters correlated with OS. A high (above median) or low (below median) mean ADC result at baseline did not correlate with OS (HR = 0.61 (95% CI: 0.23–1.60), $P = 0.31$). However, patients with a high (above median) AUC_{low} at baseline had reduced OS (HR 3.67 (95% CI: 1.23–10.9), $P = 0.012$; Figure 6A).

Of note, all six patients who progressed and died before completion of three cycles of sunitinib therapy (and therefore did not have the second MRI study) also had high AUC_{low} values at baseline.

The mean ADC and AUC_{low} after three treatment cycles were also analysed in this way and did not predict OS (HR = 0.49 (95% CI: 0.14–1.67), $P = 0.24$ and HR 2.28 (95% CI: 0.66–7.84), $P = 0.18$, respectively).

Treatment-related changes in mean ADC ranged from −13.8 to +32.9% (mean, $+7.8 \pm 15.4$). Treatment-related changes in AUC_{low} ranged from −54.3 to +56.4% (mean, -7.2 ± 30.8). Applying the 7.9% coefficient of reproducibility for our MRI system attained from an earlier repeatability study, 8 of the 17 treated patients had changes in primary tumour mean ADC that were greater than the coefficient of reproducibility (Miquel *et al*, 2012). However, there was no significant difference in the whole-tumour mean ADC at baseline and following three treatment cycles (Figure 5A, $P = 0.23$) and no correlation between the percentage change in whole-tumour mean ADC with treatment and OS (HR = 1.50 (95% CI: 0.44–5.16), $P = 0.51$). After three cycles of sunitinib, there was no correlation between the percentage change in primary tumour volume and the percentage change in whole-tumour mean ADC (correlation coefficient, -0.102 , $P = 0.93$).

There was no statistically significant difference between the baseline and post three treatment cycles AUC_{low} (Figure 5B,

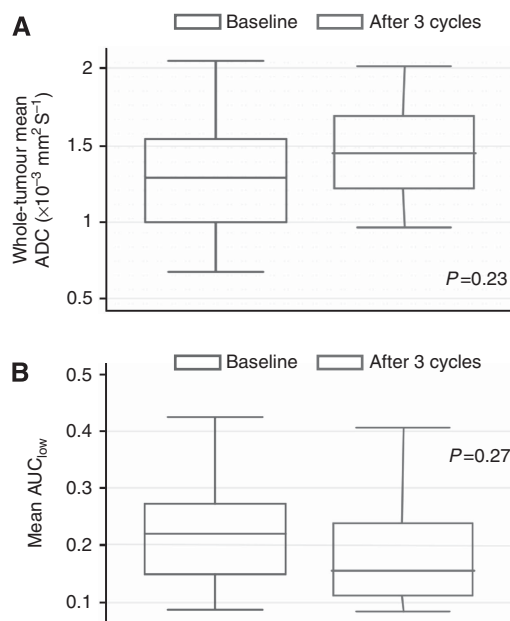


Figure 5. Box and whisker plots. Box and whisker plots showing (A) whole-tumour mean ADC and (B) mean AUC_{low} at baseline and following three cycles of sunitinib therapy. There was no statistical significance between the values ($P=0.23$ and $P=0.27$, respectively).

$P=0.27$). However, when evaluating AUC_{low} change between the baseline scan and after three cycles of therapy, those patients with a change in AUC_{low} above the median after sunitinib had a reduced OS (HR = 3.72 (95% CI: 0.98–14.21), $P=0.038$; Figure 6B); that is, those patients who had a greater-than-median positive change in the proportion of the ADC histogram curve lying below the 25th percentile point of the histogram range (an increase in AUC_{low} and a move towards a more restricted picture, more cellular tumour) had a poorer OS. The change in AUC_{low} did not correlate strongly with the change in primary tumour necrosis ($r=0.32$, $P=0.21$).

Multiphase contrast-enhanced MRI parameters. On analysis of semiquantitative MCE-MRI parameters, there was no correlation between baseline SI_{rel} , WIR, WIR_{rel} and OS ($P>0.05$ for each). The changes in these parameters following three cycles of treatment ($n=20$) were also analysed and did not predict outcome.

Metastatic deposits. The imaged DW-MRI volume contained a total of 28 measurable metastatic deposits in 13 patients at baseline – predominantly nodal sites ($n=10$), followed by IVC tumour thrombus ($n=4$), adrenal ($n=3$), subcutaneous ($n=3$), liver ($n=2$), bone ($n=2$), peritoneal ($n=1$), pancreatic ($n=1$), muscle ($n=1$) and pleural ($n=1$) metastases. Six patients had multiple deposits within the imaged volume while the remaining seven only had a single measurable deposit. Following 3 treatment cycles, 18 measurable metastatic lesions were identified, as some lesions were no longer visible/measurable ($n=5$), and 5 patients died before completion of 3 cycles (metastatic deposits = 5).

The mean ADC of metastatic deposits was measured at baseline and following sunitinib exposure, and compared with the mean ADC for the primary tumour in the same patient at each time point. At baseline, mean ADC values for the primary tumour ($1.33 \times 10^{-3} \text{ mm}^2 \text{ s}^{-1}$, s.d. 0.44) and metastatic sites ($1.27 \times 10^{-3} \text{ mm}^2 \text{ s}^{-1}$, s.d. 0.35) were not significantly different from each other ($P=0.40$). There was a positive correlation between the mean ADC of the primary tumour and metastatic sites ($r=0.607$, $P<0.001$). Following three cycles of sunitinib, the correlation between the primary tumour mean ADC and metastatic deposits persisted ($r=0.644$, $P<0.001$).

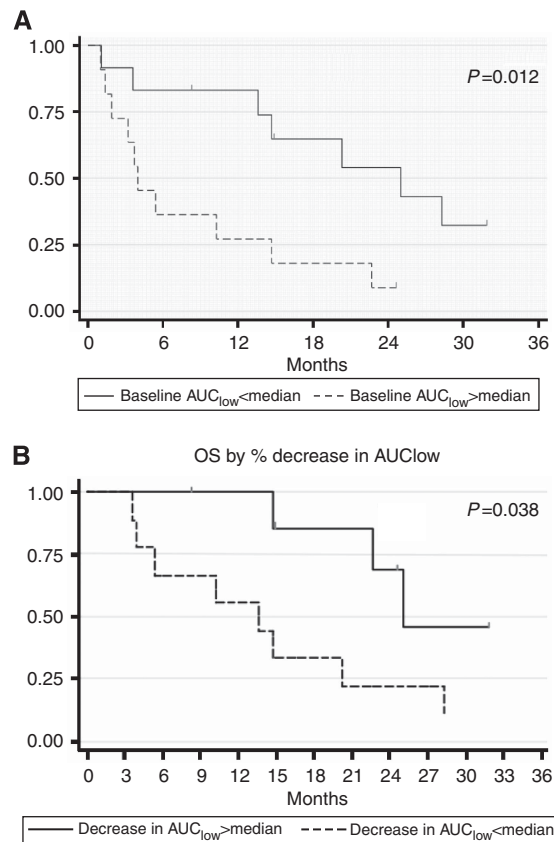


Figure 6. Overall survival correlated with AUC_{low} . (A) Baseline AUC_{low} : patients with a high (above median) AUC_{low} at baseline were compared with those who had a low baseline AUC_{low} (below median). Kaplan–Meier analysis shows a significant difference between the two groups (HR 3.67 (95% CI: 1.23–10.9), $P=0.012$). Those with higher baseline AUC_{low} values had reduced OS, that is, those patients with a larger proportion of the tumour with ADC values below the 25th percentile point of the ADC histogram at baseline had poorer OS. (B) Change in AUC_{low} between the pre- and post-treatment studies: patients with an above-median percentage change in AUC_{low} between the baseline scan and post three cycles of scan were compared with those who had a percentage change below the median. Kaplan–Meier analysis shows a significant difference between the two groups (HR = 3.72 (95% CI = 0.98–14.21), $P=0.038$). Those with a larger increase in AUC_{low} after three cycles had a reduced OS, that is, patients whose ADC histograms showed leftward shift (an increase in AUC_{low} and a move towards a more restricted picture) had a poorer OS (AUC_{low} = proportion of the tumour with ADC values lying below the 25th percentile of the ADC histogram).

Multiphase contrast-enhanced MRI analysis was not possible for the majority of metastases due to difficulties in accurate lesion identification and ROI placement in relation to the coronal acquisition.

DISCUSSION

There is an urgent need for surrogate markers to reliably predict the probable response early in the course of targeted therapy in mRCC. To date, attempts with other imaging techniques have shown variable success (Hahn *et al*, 2008; Nathan *et al*, 2010; Thiam *et al*, 2010; Smith *et al*, 2010a,b; Goh *et al*, 2011; Han *et al*, 2010; Kayani *et al*, 2011; Krajewski *et al*, 2011; Smith *et al*, 2011). Size and CT attenuation criteria have been reported to predict outcome better than RECIST criteria; however, this

requires intravenous contrast material, which may not be given in up to a third of patients with mRCC (Nathan *et al*, 2010).

Our work evaluates the role of sequential DW- and MCE-MRI as potential surrogate markers of outcome in untreated mRCC patients at baseline and following three cycles of sunitinib. Although biomarkers obtained following a shorter treatment period, for example, 2 weeks, may provide very early response data, they would not identify those patients who develop early resistance to sunitinib therapy. By performing imaging after approximately 4 months of treatment, we hoped to identify this early resistance sooner than it is detected on CT (typically following 10 months of treatment). Diffusion-weighted MRI may be a marker of apoptosis and tumour cellularity (Thoeny *et al*, 2005; Hamstra *et al*, 2007; Patterson *et al*, 2008; Padhani *et al*, 2009) and therefore drug activity. Dynamic CE MRI parameters have been proposed as pharmacodynamic biomarkers in patients on anti-angiogenic therapy (Morgan *et al*, 2003; Stevenson *et al*, 2003; Liu *et al*, 2005; Mross *et al*, 2005; Flaherty *et al*, 2008; Hahn *et al*, 2008; Notohamiprodjo *et al*, 2010).

Most tumours in our study were large heterogeneous lesions with cystic and solid components and evidence of intratumoural haemorrhage on T_1 -weighted imaging (Figures 3 and 4). Histologically and at a molecular level, mRCC shows considerable heterogeneity (Gerlinger *et al*, 2012). Pathological sampling can reveal cytoplasmic and nuclear grade variability within the same tumour, whereas specific clones are found using DNA sequencing techniques (Kanamaru *et al*, 1996). This may explain the greater variation seen on imaging than in other, more homogeneous, tumour types. The relatively large size of renal tumours also allows more phenotypic diversity. These factors may account for some of the difficulties encountered in attempts to develop surrogate markers of response in mRCC, both at functional imaging and at molecular levels.

In our cohort, baseline whole-tumour mean ADC did not predict outcome. Although measurable changes occurred above the level of repeatability of our system with sunitinib therapy in 47% of patients, changes in mean ADC were also not predictive of OS.

As a further exploratory assessment, we went on to specifically evaluate the tissues of initially low ADC (the proportion of the tumour with ADC values lying below the 25th percentile point of the ADC histogram – AUC_{low}), representing the most restricted and probably the most cellular part of the primary tumour. Analysis of this portion of the histogram demonstrated changes in the spread of ADC values, which may reflect dynamic intratumoural changes following treatment. The lower portion of the ADC histogram has also been evaluated in other tumour types (Nowosielski *et al*, 2011; Pope *et al*, 2011) where histogram-derived parameters have been shown to relate to PFS and treatment response. In our study, KM analysis showed a statistically significant correlation between OS and (i) high (above median) baseline AUC_{low} and (ii) the percentage change in AUC_{low} with treatment (above and below median). Patients with a greater proportion of tumour lying below the 25th percentile point of the whole-tumour ADC histogram, that is, a greater proportion of restricted tissue, had reduced survival. In addition, patients with a greater-than-median positive change in AUC_{low} (i.e., an increase in the proportion of restricted tissue) had reduced survival, whereas those with a decrease in AUC_{low} had prolonged survival. A reduction in AUC_{low} (due to an increase in the ADC of these tissues with treatment) is postulated to be caused by cellular breakdown and apoptosis associated with treatment response. Although the targeted effects of sunitinib are against receptor tyrosine kinases, the off-target effects of the drug are unclear and pre-clinical work shows that apoptosis does occur (Xin *et al*, 2009). These changes may help to identify patients who respond to sunitinib but who are unable to have intravenous contrast media precluding the use of combined size and attenuation criteria on CT.

To our knowledge, only one other group has published data concerning DW-MRI in mRCC patients treated with sunitinib (Desar *et al*, 2011). Desar *et al* (2011) evaluated the mean ADC values within a single slice through the primary renal tumour at three time points (baseline, day 3 and day 10 of the first treatment cycle) in ten patients treated with sunitinib. They demonstrated chemotherapy-related changes in mean ADC, which were attributed to cellular swelling at day 3 (increased mean ADC) followed by tissue dehydration by day 10 (reduction in mean ADC compared with day 3). These ADC changes did not correlate with DCE-MRI parameters or response measures in their patient group. Our study differs from that of Desar *et al* (2011) in evaluating the whole-tumour volume, considering both whole-tumour mean ADC values, but also histogram analysis of the mean ADC within each voxel occupied by tumour. This analysis provides greater detail regarding the tumour microenvironment and is potentially more sensitive to treatment-related changes. It is also important to note that the study performed by Desar *et al* (2011) evaluated patients while on treatment with sunitinib, whereas our study evaluates changes in the primary tumour 10 ± 2 days after completion of three cycles of sunitinib therapy (i.e., off therapy). There is a very labile relationship between the timing of imaging relative to the treatment patients are receiving; as Desar *et al* (2011) showed, mean ADC changes at different time points within the same treatment cycle and it is likely to be that further changes occur when patients come off treatment. Indeed, we know that patients treated with neoadjuvant sunitinib have been shown to progress during the treatment break before surgery (Powles *et al*, 2011).

Our study found a positive correlation between the mean ADC in the metastatic deposits and primary renal tumour in individual patients before and after sunitinib treatment. This suggests that there is a similarity in treatment response between the primary sites and metastatic deposits. This is an important finding for biomarker research in mRCC and supports the hypothesis that molecular markers taken from primary renal tissue may be representative of the metastatic sites.

Previous studies using DCE-MRI have suggested a correlation between high pre-treatment K_{trans} and PFS (Flaherty *et al*, 2008; Hahn *et al*, 2008), and treatment-related reduction in K_{trans} and PFS (Flaherty *et al*, 2008), whereas other groups have shown no significant correlation between K_{trans} , k_{ep} and response (Desar *et al*, 2011). The semiquantitative parameters used in our study are more easily employed in everyday clinical practice than quantitative measures such as K_{trans} , and they have been shown to be useful in the assessment of tumour biology in other cancer types (Mussurakis *et al*, 1997; Bernardin *et al*, 2012). However, they have not been evaluated in response assessment.

We did not find any correlation between OS and semiquantitative MCE-MRI parameters within the primary renal tumour (at baseline, post three cycles or treatment-related change) using a simple and widely available technique. Failure of MCE-MRI to predict clinical outcome in our patient group may, in part, be related to the marked heterogeneity of mRCC and subjective selection of the most enhancing region of tumour for ROI placement, or may be related to the type of analysis performed. As WIR is defined using the maximum point of enhancement over the duration of the dynamic acquisition, this limits the ability of this technique to distinguish between very vascular tumours, which tend to enhance early and reach a maximum soon after contrast injection, and persistent, slowly enhancing tumours, which may reach maximal enhancement towards the end of the acquisition.

There are a number of limitations to our study. The prospective phase II clinical trial was powered to address the efficacy of upfront sunitinib and the imaging substudy was a secondary endpoint, optional for patients and exploratory in nature, resulting in a relatively small cohort. This may have influenced some of the results, especially those where there was a trend towards

significance. Sequential imaging was not possible in a proportion of patients (six patients; 26%) owing to disease progression resulting in death. The cohort therefore under represents patients with primary refractory disease. Imaging was performed at specific time points to fit in with events in the clinical trial. However, results may have been different if the MRI scan were performed at an earlier time point and more patients may have achieved the post-treatment MRI scan if this had been done following cycle 1. Results may have also been different if the second imaging study had been performed on treatment at the end of a cycle rather than off treatment. Progression-free survival was not considered to be a reliable endpoint for this study, as a high proportion of patients have radiological progression during the treatment break for surgery. Intra- and interobserver variability have not been evaluated in this study.

CONCLUSION

In conclusion, DW-MRI provides a potential biomarker, AUC_{low} , for OS in mRCC treated with sunitinib. A high baseline AUC_{low} and a greater-than-median increase in AUC_{low} with treatment show a statistically significant correlation with reduced OS. Although our cohort is too small to suggest cut-off values for these parameters, with further validation in a larger study AUC_{low} could act as a threshold for treatment change in this patient group. Furthermore, a correlation between ADC change in the primary tumour and metastases exists in individual patients, an important finding for future biomarker research.

ACKNOWLEDGEMENTS

MEM is partly funded (20%) by the Barts and the London National Institute for Health Research (NIHR) Cardiovascular Biomedical Research Unit.

CONFLICT OF INTEREST

TP – education grant, advisory role from Pfizer, AZ, GSK and Novartis; advisory role for GE Roche and Genetech. AGR – honoraria and travel support for educational role, Novartis; travel support for educational role, Guerbet. All other authors declare no conflict of interest.

REFERENCES

- Bernardin L, Dilks P, Liyanage S, Miquel ME, Sahdev A, Rockall A (2012) Effectiveness of semi-quantitative multiphase dynamic contrast-enhanced MRI as a predictor of malignancy in complex adnexal masses: radiological and pathological correlation. *Eur Radiol* **22**: 880–890.
- Desar IM, ter Voert EG, Hambroek T, van Asten JJ, van Spronsen DJ, Mulders PF, Heerschap A, van der Graaf WT, van Laarhoven HW, van Herpen CM (2011) Functional MRI techniques demonstrate early vascular changes in renal cell cancer patients treated with sunitinib: a pilot study. *Cancer Imaging* **11**: 259–265.
- Flaherty KT, Rosen MA, Heitjan DF, Gallagher ML, Schwartz B, Schnall MD, O'Dwyer PJ (2008) Pilot study of DCE-MRI to predict progression-free survival with sorafenib therapy in renal cell carcinoma. *Cancer Biol Ther* **7**: 496–501.
- Gerlinger M, Rowan AJ, Horswell S, Math M, Larkin J, Endesfelder D, Gronroos E, Martinez P, Matthews N, Stewart A, Tarpey P, Varela I, Phillimore B, Begum S, McDonald NQ, Butler A, Jones D, Raine K, Latimer C, Santos CR, Nohadani M, Eklund AC, Spencer-Dene B, Clark G, Pickering L, Stamp G, Gore M, Szallasi Z, Downward J, Futreal PA, Swanton C (2012) Intratumor heterogeneity and branched evolution revealed by multiregion sequencing. *N Engl J Med* **366**: 883–892.
- Goh V, Ganeshan B, Nathan P, Juttla JK, Vinayan A, Miles KA (2011) Assessment of response to tyrosine kinase inhibitors in metastatic renal cell cancer: CT texture as a predictive biomarker. *Radiology* **261**: 165–171.
- Griffin N, Grant LA, Bharwani N, Sohaib SA (2009) Computed tomography in metastatic renal cell carcinoma. *Semin Ultrasound CT MR* **30**: 359–366.
- Hahn OM, Yang C, Medved M, Karczmar G, Kistner E, Karrison T, Manchen E, Mitchell M, Ratain MJ, Stadler WM (2008) Dynamic contrast-enhanced magnetic resonance imaging pharmacodynamic biomarker study of sorafenib in metastatic renal carcinoma. *J Clin Oncol* **26**: 4572–4578.
- Hamstra DA, Rehemtulla A, Ross BD (2007) Diffusion magnetic resonance imaging: a biomarker for treatment response in oncology. *J Clin Oncol* **25**: 4104–4109.
- Han KS, Jung DC, Choi HJ, Jeong MS, Cho KS, Joung JY, Seo HK, Lee KH, Chung J (2010) Pretreatment assessment of tumor enhancement on contrast-enhanced computed tomography as a potential predictor of treatment outcome in metastatic renal cell carcinoma patients receiving antiangiogenic therapy. *Cancer* **116**: 2332–2342.
- Harry VN, Semple SI, Gilbert FJ, Parkin DE (2008) Diffusion-weighted magnetic resonance imaging in the early detection of response to chemoradiation in cervical cancer. *Gynecol Oncol* **111**: 213–220.
- Jung SH, Heo SH, Kim JW, Jeong YY, Shin SS, Soung MG, Kim HR, Kang HK (2011) Predicting response to neoadjuvant chemoradiation therapy in locally advanced rectal cancer: diffusion-weighted 3 tesla MR imaging. *J Magn Reson Imaging* **35**(1): 110–116.
- Kanamaru H, Muranaka K, Mori H, Akino H, Arai Y, Okada K (1996) Analysis of histological heterogeneity in renal cell carcinoma: tumor size-related histological change and its prognostic significance. *Int J Urol* **3**: 256–260.
- Kayani I, Avril N, Bomanji J, Chowdhury S, Rockall A, Sahdev A, Nathan P, Wilson P, Shamash J, Sharpe K, Lim L, Dickson J, Ell P, Reynolds A, Powles T (2011) Sequential FDG-PET/CT as a biomarker of response to Sunitinib in metastatic clear cell renal cancer. *Clin Cancer Res* **17**: 6021–6028.
- Koh DM, Collins DJ (2007) Diffusion-weighted MRI in the body: applications and challenges in oncology. *AJR Am J Roentgenol* **188**: 1622–1635.
- Kontovinis LF, Papazisis KT, Touplikioti P, Andreadis C, Mouratidou D, Kortsaris AH (2009) Sunitinib treatment for patients with clear-cell metastatic renal cell carcinoma: clinical outcomes and plasma angiogenesis markers. *BMC Cancer* **9**: 82.
- Krajewski KM, Guo M, Van den Abbeele AD, Yap J, Ramaiya N, Jagannathan J, Heng DY, Atkins MB, McDermott DF, Schutz FA, Pedrosa I, Choueiri TK (2011) Comparison of four early posttherapy imaging changes (EPTIC; RECIST 1.0, tumor shrinkage, computed tomography tumor density, Choi criteria) in assessing outcome to vascular endothelial growth factor-targeted therapy in patients with advanced renal cell carcinoma. *Eur Urol* **59**: 856–862.
- Kyriazi S, Collins DJ, Messiou C, Pennert K, Davidson RL, Giles SL, Kaye SB, Desouza NM (2011) Metastatic ovarian and primary peritoneal cancer: assessing chemotherapy response with diffusion-weighted MR imaging—value of histogram analysis of apparent diffusion coefficients. *Radiology* **261**: 182–192.
- Liu G, Rugo HS, Wilding G, McShane TM, Evelhoch JL, Ng C, Jackson E, Kelcz F, Yeh BM, Lee Jr FT, Charnsangavej C, Park JW, Ashton EA, Steinfeldt HM, Pithavala YK, Reich SD, Herbst RS (2005) Dynamic contrast-enhanced magnetic resonance imaging as a pharmacodynamic measure of response after acute dosing of AG-013736, an oral angiogenesis inhibitor, in patients with advanced solid tumors: results from a phase I study. *J Clin Oncol* **23**: 5464–5473.
- Miquel ME, Scott AD, Macdougall ND, Boubertakh R, Bharwani N, Rockall AG (2012) *In vitro* and *in vivo* repeatability of abdominal diffusion-weighted MRI. *Br J Radiol* **85**: 1507–1512.
- Morgan B, Thomas AL, Drevs J, Hennig J, Buchert M, Jivan A, Horsfield MA, Mross K, Ball HA, Lee L, Mietlowski W, Fuxuis S, Unger C, O'Byrne K, Henry A, Cherryman GR, Laurent D, Dugan M, Marme D, Steward WP (2003) Dynamic contrast-enhanced magnetic resonance imaging as a biomarker for the pharmacological response of PTK787/ZK 222584, an inhibitor of the vascular endothelial growth factor receptor tyrosine kinases, in patients with advanced colorectal cancer and liver metastases: results from two phase I studies. *J Clin Oncol* **21**: 3955–3964.

- Motzer RJ, Hutson TE, Tomczak P, Michaelson MD, Bukowski RM, Oudard S, Negrier S, Szczylik C, Pili R, Bjarnason GA, Garcia-del-Muro X, Sosman JA, Solska E, Wilding G, Thompson JA, Kim ST, Chen I, Huang X, Figlin RA (2009) Overall survival and updated results for sunitinib compared with interferon alfa in patients with metastatic renal cell carcinoma. *J Clin Oncol* **27**: 3584–3590.
- Motzer RJ, Hutson TE, Tomczak P, Michaelson MD, Bukowski RM, Rixe O, Oudard S, Negrier S, Szczylik C, Kim ST, Chen I, Bycott PW, Baum CM, Figlin RA (2007) Sunitinib versus interferon alfa in metastatic renal-cell carcinoma. *N Engl J Med* **356**: 115–124.
- Mross K, Dreys J, Muller M, Medinger M, Marme D, Hennig J, Morgan B, Lebowhl D, Masson E, Ho YY, Gunther C, Laurent D, Unger C (2005) Phase I clinical and pharmacokinetic study of PTK/ZK, a multiple VEGF receptor inhibitor, in patients with liver metastases from solid tumours. *Eur J Cancer* **41**: 1291–1299.
- Mussurakis S, Buckley DL, Horsman A (1997) Dynamic MR imaging of invasive breast cancer: correlation with tumour grade and other histological factors. *Br J Radiol* **70**: 446–451.
- Nathan PD, Vinayan A, Stott D, Juttla J, Goh V (2010) CT response assessment combining reduction in both size and arterial phase density correlates with time to progression in metastatic renal cancer patients treated with targeted therapies. *Cancer Biol Ther* **9**: 15–19.
- Notohamiprodjo M, Sourbron S, Staehler M, Michaely HJ, Attenberger UI, Schmidt GP, Boehm H, Horng A, Glaser C, Stief C, Reiser MF, Herrmann KA (2010) Measuring perfusion and permeability in renal cell carcinoma with dynamic contrast-enhanced MRI: a pilot study. *J Magn Reson Imaging* **31**: 490–501.
- Nowosielski M, Recheis W, Goebel G, Guler O, Tinkhauser G, Kostron H, Schocke M, Gotwald T, Stockhammer G, Hutterer M (2011) ADC histograms predict response to anti-angiogenic therapy in patients with recurrent high-grade glioma. *Neuroradiology* **53**: 291–302.
- Padhani AR, Liu G, Koh DM, Chenevert TL, Thoeny HC, Takahara T, Dzik-Jurasz A, Ross BD, Van Cauteren M, Collins D, Hammoud DA, Rustin GJ, Taouli B, Choyke PL (2009) Diffusion-weighted magnetic resonance imaging as a cancer biomarker: consensus and recommendations. *Neoplasia* **11**: 102–125.
- Patterson DM, Padhani AR, Collins DJ (2008) Technology insight: water diffusion MRI—a potential new biomarker of response to cancer therapy. *Nat Clin Pract Oncol* **5**: 220–233.
- Pope WB, Lai A, Mehta R, Kim HJ, Qiao J, Young JR, Xue X, Goldin J, Brown MS, Nghiemphu PL, Tran A, Cloughesy TF (2011) Apparent diffusion coefficient histogram analysis stratifies progression-free survival in newly diagnosed bevacizumab-treated glioblastoma. *AJNR Am J Neuroradiol* **32**: 882–889.
- Powles T, Blank C, Chowdhury S, Horenblas S, Peters J, Shamash J, Sarwar N, Boleti E, Sahdev A, O'Brien T, Berney D, Beltran L, Nathan P, Haanen J, Bex A (2011) The outcome of patients treated with sunitinib prior to planned nephrectomy in metastatic clear cell renal cancer. *Eur Urol* **60**: 448–454.
- Rosset A, Spadola L, Ratib O (2004) OsiriX: an open-source software for navigating in multidimensional DICOM images. *J Digit Imaging* **17**: 205–216.
- Smith AD, Lieber ML, Shah SN (2010a) Assessing tumor response and detecting recurrence in metastatic renal cell carcinoma on targeted therapy: importance of size and attenuation on contrast-enhanced CT. *AJR Am J Roentgenol* **194**: 157–165.
- Smith AD, Shah SN, Rini BI, Lieber ML, Remer EM (2010b) Morphology, Attenuation, Size, and Structure (MASS) criteria: assessing response and predicting clinical outcome in metastatic renal cell carcinoma on antiangiogenic targeted therapy. *AJR Am J Roentgenol* **194**: 1470–1478.
- Smith AD, Shah SN, Rini BI, Lieber ML, Remer EM (2011) Utilizing pre-therapy clinical schema and initial CT changes to predict progression-free survival in patients with metastatic renal cell carcinoma on VEGF-targeted therapy: A preliminary analysis. *Urol Oncol* **31**(7): 1283–1291.
- Stevenson JP, Rosen M, Sun W, Gallagher M, Haller DG, Vaughn D, Giantonio B, Zimmer R, Petros WP, Stratford M, Chaplin D, Young SL, Schnall M, O'Dwyer PJ (2003) Phase I trial of the antivascular agent combretastatin A4 phosphate on a 5-day schedule to patients with cancer: magnetic resonance imaging evidence for altered tumor blood flow. *J Clin Oncol* **21**: 4428–4438.
- Thiam R, Fournier LS, Trinquart L, Medioni J, Chatellier G, Balvay D, Escudier B, Dromain C, Cuenod CA, Oudard S (2010) Optimizing the size variation threshold for the CT evaluation of response in metastatic renal cell carcinoma treated with sunitinib. *Ann Oncol* **21**: 936–941.
- Thoeny HC, De Keyzer F, Vandecaveye V, Chen F, Sun X, Bosmans H, Hermans R, Verbeken EK, Boesch C, Marchal G, Landuyt W, Ni Y (2005) Effect of vascular targeting agent in rat tumor model: dynamic contrast-enhanced versus diffusion-weighted MR imaging. *Radiology* **237**: 492–499.
- Xin H, Zhang C, Herrmann A, Du Y, Figlin R, Yu H (2009) Sunitinib inhibition of Stat3 induces renal cell carcinoma tumor cell apoptosis and reduces immunosuppressive cells. *Cancer Res* **69**: 2506–2513.

This work is published under the standard license to publish agreement. After 12 months the work will become freely available and the license terms will switch to a Creative Commons Attribution-NonCommercial-Share Alike 3.0 Unported License.